

Epigenetic Reprogramming and Non-Homologous Chromosomal Contact in Chemotherapy-Resistant Favorable-Histology Wilms Tumor

Authors

Andrew M. Fleming, MD^{1,2,#}, Carolyn M. Jablonowski, PhD^{2,#}, Hongjian Jin³, PhD, Surbhi Sona, PhD³, Ha Won Lee, PhD⁴, Karissa M. Dieseldorff Jones, PhD⁵, Changde Cheng, PhD⁵, Beisi Xu, PhD³, Chris Morton BS, MBA², Mary A. Woolard, BS², Prahalathan Pichavaram, PhD², Daniel Gehle, MD^{1,2}, Sivaraman Natarajan, PhD⁵, Kiran Kodali⁶, Vishwajeeth Pagala⁶, Anthony High, PhD⁶, Yogesh Kumar³, Ti Cheng Chang³, John Easton, PhD³, Scott R Olsen, MS⁷, Geoffrey Neale, PhD⁷, Emilia M. Pinto, PhD⁸, Jerold E. Rehg, DVM⁸, Laura Janke, DVM, PhD⁸, Teresa Santiago, MD⁸, Rani George, MD, PhD^{9,10}, Xiaotu Ma, PhD⁵, Gerard P. Zambetti, PhD⁸, Andrew M. Davidoff, MD^{1,2}, Taosheng Chen, PhD⁴, Gang Wu, PhD³, Xiang Chen, PhD⁵, Jun Yang, MBBS, PhD², Andrew J. Murphy, MD^{1,2*}

¹The University of TN Health Science Center, Department of Surgery, Memphis, TN

²St. Jude Children's Research Hospital, Department of Surgery, Memphis, TN

³St. Jude Children's Research Hospital, Center for Applied Bioinformatics, Memphis, TN

⁴St. Jude Children's Research Hospital, Department of Chemical Biology and Therapeutics, Memphis, TN

⁵St. Jude Children's Research Hospital, Department of Computational Biology, Memphis, TN

⁶St. Jude Children's Research Hospital, Center for Proteomics and Metabolomics, Memphis, TN

⁷St. Jude Children's Research Hospital, Hartwell Center for Biotechnology, Memphis, TN

⁸St. Jude Children's Research Hospital, Department of Pathology, Memphis, TN

⁹Dana-Farber/Boston Children's Cancer and Blood Disorders Center, Boston, MA

¹⁰Harvard Medical School, Boston, MA

The current analysis demonstrates a “cancer stem cell” phenotype in chemotherapy-resistant favorable histology Wilms tumor resulting from cancer cell plasticity / epigenetic reprogramming rather than selection of a minor subclone.

(Words: 300/300)

Background

Chemotherapy resistance in the favorable histology Wilms Tumor (FHWT) patient derived xenograft (WTPDX), KT-47, associated with enrichment of the microRNA processor *LIN28B*, *MYCN*, and *ABCB1*. This analysis identified mechanisms underlying these events.

Methods

Whole genome sequencing (WGS), CUT&TAG, single nuclear multiome assay for transposase-accessible chromatin (ATAC) with ATAC-seq, HiC, and 2D cell culture were used to evaluate changes associated with resistance.

Results

Following K-means clustering of single nuclear gene expression (GEX) and ATAC signatures, *LIN28B* ATAC promoter sum data indicated that chromatin accessibility at the *LIN28B* promoter correlated with *LIN28B* GEX in the KT-47 resistance 1 (R1) sample among nuclei representing fetal kidney metanephric cells (Figure 1A). Given ATAC motif analysis suggested chromatin looping in the upregulation of *LIN28B*, we performed HiC to comprehensively analyze chromatin interactions in KT-47. HiC did not demonstrate differences in chromatin interactions surrounding the *LIN28B* locus (chr6q16.3) or in chromosome 6 when comparing the KT-47 pretreatment and KT-47R1 models. However, evidence of *MYCN* copy number gain in KT-47R was detected on HiC and confirmed on Multiplex Ligation-dependent Probe Amplification (MLPA) and CONSERTING algorithm analysis of whole genome sequencing data (Figure 1B). HiC also demonstrated an inter-chromosomal interaction between chromosomes 1p32.3 and 7q21 immediately upstream of the *ABCB1* locus, chr1:53,700,000(*GLIS1*) vs chr7:87,605,000(*ABCB1*; Figure 1C) present in the KT-47R model but not the pretreatment model. A chromosomal translocation at this location was ruled out using WGS data and cytogenetic approaches (FISH), indicating that this interaction constituted a non-homologous chromosomal contact between chromosomes 1p32.3 and 7q21 rather than a translocation. Forced expression of wild type *MYCN* and mutant *MYCN* p.P44L in WiT49 Wilms tumor cells resulted in upregulation of *LIN28B* (Figure 1D).

Conclusions

The current analysis demonstrates a “cancer stem cell” phenotype resulting from cancer cell plasticity / epigenetic reprogramming rather than selection of a minor subclone.

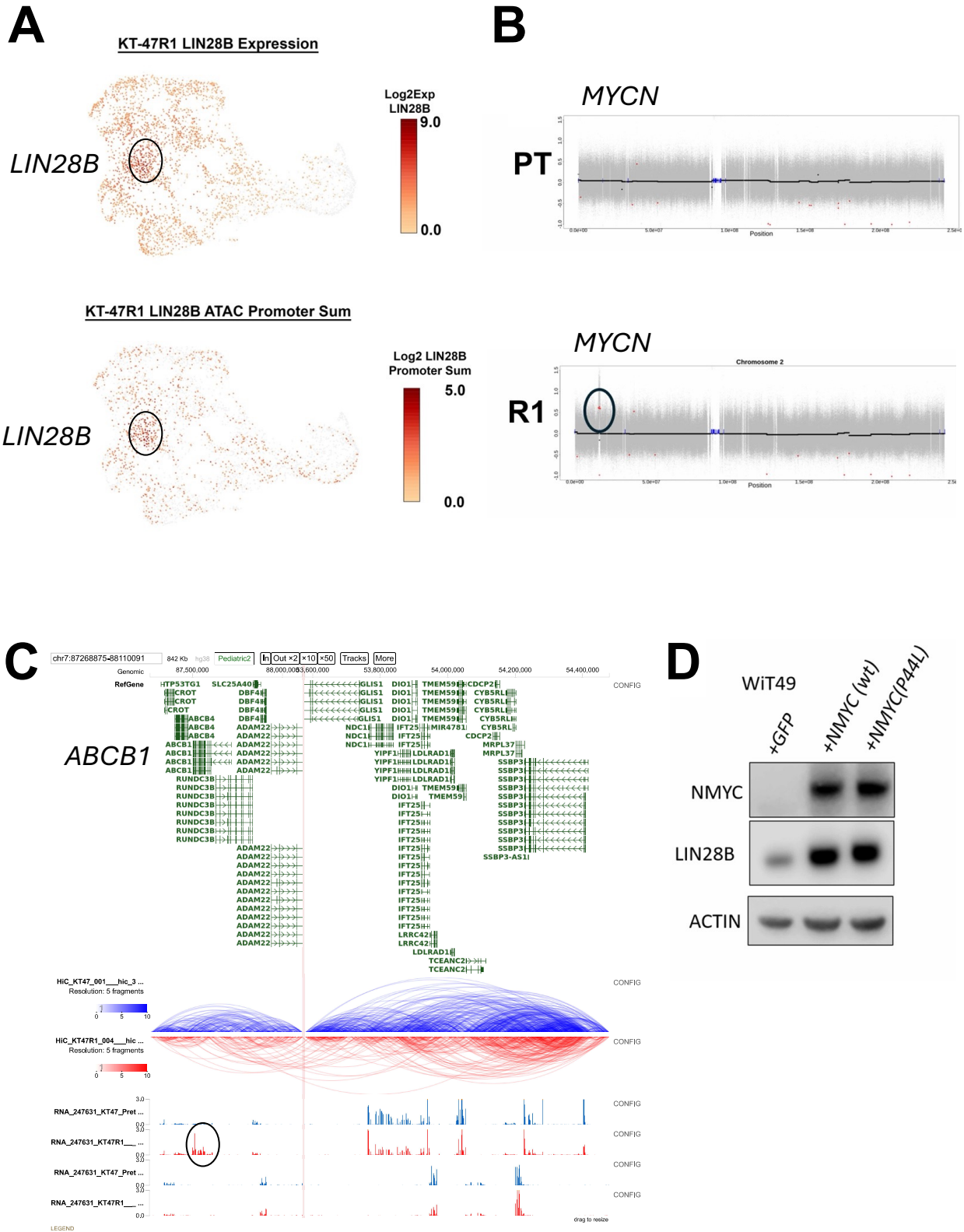


Figure 1. (A) *LIN28B* was robustly expressed in the KT-47R1 clusters that were inferred to represent fetal kidney (FK) metanephric cells (marked with ovals) but not in the skeletal

muscle or stroma cluster as determined by gene expression (GEX). *LIN28B* expression was strongest in the area which contained both FK metanephric and FK ureteric bud cells as determined by ATAC data. *LIN28B* ATAC promoter sum data indicate that chromatin accessibility at the *LIN28B* promoter correlated with *LIN28B* GEX in the KT-47R1 sample. The overall architecture of the plot was created using a UMAP projection. **(B)** CONSERVING algorithm analysis of whole genome sequencing data also confirmed copy number gain of *MYCN* in KT-47 pre-resistance, and in KT-47R1 and KT-47R2 (red dots within ovals indicate copy number gain of *MYCN*). **(C)** HiC identified an inter-chromosomal interaction between chromosomes 1p32.3 (*GLIS1* locus) and 7q21 (*ABCB1* locus). Arch plots of topologically associated domains (TAD, scale indicates degree of interaction) demonstrate this interaction is present in KT-47R (red lines, interaction shown by dashed lines; point of maximal interaction immediately upstream of *ABCB1*) but not in KT-47 Pretreatment (KT-47PT, blue lines). **(D)** Forced expression of wild type *MYCN* and mutant *MYCN* p.P44L (mutation seen in Wilms tumor) in Wit49 Wilms tumor cells resulted in upregulation of *LIN28B*.